Estimating vector magnitude from its direction and derivative, with application to bearing-only SLAM filter problem

Elias Bjørne* Jeff Delaune † Tor Arne Johansen*

***Abstract*— For some problems, such as monocular visual odometry (VO), vector measurements are given with unknown magnitude. In VO, the magnitude can be found by recognizing features with known position, or with an extra sensor such as an altimeter. This article presents a nonlinear observer that uses the derivative of the vector as an additional measurement for estimating the magnitude of a vector. For the VO example, this means that the velocity can be estimated by fusing the normalized velocity vector with acceleration measurements. The observer exploits the fact that the dynamics of the normalized vector is dependent on the magnitude of the vector. The observer employs methods from nonlinear/adaptive estimation; filters the unit vector on the unit sphere, and retrieves the magnitude of the vector. The observer is shown to be uniformly semi-globally asymptotically (USGAS) stable and uniformly exponentially stable (UES) in a defined region. The observer is applied to the bearing-only SLAM filter problem as an example.**

***Index Terms*— Nonlinear observer, skew-symmetric system, direction measurement, bearing, simultanous localization and mapping, ego-motion estimation**

I. Introduction

In some estimation problems, the measurements available can be of a vector with unknown magnitude, which we then want to estimate. This is especially relevant for bearing-only localization or tracking, in which the scale from a monocular camera is ambigous without any further knowledge or sensors [1]. In other words, the direction of the velocity can be measured [2], but not the magnitude. In the simultaneous localization and mapping (SLAM) literature, there are many solutions to fusing bearing mesurments with different sensors and assumptions to find the scale, howerver, there is a lack of theoretical stability proof on many of the most popular solutions, which either use a version of extended Kalman filter (EKF) [3], [4], probability graphs [5] or particle filters [6]. These are optimization based solutions often resulting in accurate estimates, however, they are computationally demanding, and guaranteed stability can often be difficult if not impossible to acquire. This has given some motivation to attack the SLAM filter problem with nonlinear observers (NLO), as they usually have complimentary characteristics to the mentioned methods: defined stability traits with defined region of attraction, low computational cost, although lacking optimality when they handle noisy measurements [7], [8]. Other NLO approaches for the SLAM problem are presented in [9]–[11], where [10] and [11] assume velocity measurement or biased velocity measurement, while in [9] the authors present a NLO for fusing measurements from the homography with IMU data.

In this article we present a novel observer for estimating the magnitude of a time varying vector. We prove that if we assume a lower bound on the magnitude of the vector, and a persistently exciting vector measurement, the vector magnitude observer is uniformly semi-globally asymptotically stable (USGAS) and uniformly locally exponentially stable (ULES) and will hence estimate the magnitude of the vector. We employ the vector magnitude observer to the bearing-only SLAM problem with AHRS measurements, and this also demonstrates two instances of the vector magnitude observer working in cascade; once for velocity and once for range to landmark estimation.

In Section II we present notation and preliminaries. Section III presents the stability analysis of the observer. Section IV presents how the the novel observer can be applied to the bearing-only SLAM filter problem, with related simulations. Section V concludes the work.

II. Notation and previous work

A. Notation

Scalars are in lower case a, x, ω; vectors are lower case bold $\boldsymbol{a}, \boldsymbol{x}, \boldsymbol{\omega}$; sets are upper case A, X, Ω; matrices are bold upper case $\boldsymbol{A}, \boldsymbol{X}, \boldsymbol{\Omega}$. The 0 denotes the scalar zero, while $\mathbf{0}$ is the matrix zero where dimensions are implicitly given by the context. The matrix $\boldsymbol{I}$ is the identity matrix, and size is given by context. The accents $\hat{\bullet}, \tilde{\bullet}, \dot{\bullet}, \bar{\bullet}, \underline{\bullet}$, denotes estimate, estimate error, time derivative, upper bound and lower bound respectively. Some common mathematical expressions which will be used are: The Euclidean norm for vectors and frobenius norm for matrices, $\| \bullet \|$, absolute value, $| \bullet |$ and the transpose, $\bullet^\top$. The representation of index sets will be done with $\{1, ..., n\} = \{x \in \mathbb{Z} | x \leq n\}$.
A vector is said to be on the unit sphere $\boldsymbol{u}_\bullet \in \mathcal{S}^3 = \{\boldsymbol{u}_\bullet \in \mathbb{R}^3 | \ \|\boldsymbol{u}_\bullet\| = 1\}$. and will stay on the unit sphere if its derivative is always orthogonal to itself $\boldsymbol{u}_\bullet(t + t_0) \in \mathcal{S}^3 \ \forall t + t_0 \iff \{\boldsymbol{u}_\bullet(t) : \mathbb{R} \to \mathbb{R}^3 | \ \|\boldsymbol{u}_\bullet(t_0)\| = 1, \ \boldsymbol{u}_\bullet(t_0 + t)^\top \dot{\boldsymbol{u}}_\bullet(t_0 + t) = 0 \ \forall t \geq 0\}$. A vector can be represented in different coordinate systems, the representation is denoted with the superscripts $\bullet^b, \bullet^n$ which represents the body-fixed and earth-fixed (inertial) coordinate systems, and will be

*Elias Bjørne and Tor Arne Johansen are with the Department of Engineering Cybernetics, Norwegian University of Science and Technology (NTNU), NO-7491 Trondheim, Norway. (Email: elias.bjorne@itk.ntnu.no, tor.arne.johansen@itk.ntnu.no)
and are associated with the NTNU Centre for Autonomous Marine Operations and Systems.
†Jeff Delaune is with Computer Vision Group at Jet Propulsion Labratory, NASA, California Institute of Technology. (Email: Jeff.H.Delaune@jpl.nasa.gov

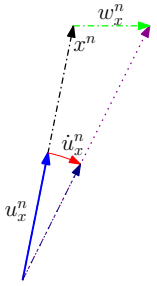

Fig. 1: Vector dynamics in inertial-frame

called body-frame and inertial-frame. Lower case will denote the indices of a landmark, vector or matrix $\bullet_i$ and $\bullet_{ij}$.

Rotation is the attitude change between two coordinate systems. Rotation from coordinate system b to n can be represented with a rotation matrix
$\boldsymbol{\mathcal{R}}_{nb} \in \{\mathbb{R}^{3\times 3} |\ \boldsymbol{\mathcal{R}}_{nb}\boldsymbol{\mathcal{R}}_{nb}^\top = \boldsymbol{I},\ det(\boldsymbol{\mathcal{R}}_{nb}) = 1\}$
which means $\boldsymbol{\mathcal{R}}_{nb} \in SO(3)$. The rotation vector transformation is calculated by $\boldsymbol{x}^n = \boldsymbol{\mathcal{R}}_{nb}\boldsymbol{x}^b$. The cross product is presented in matrix form $\boldsymbol{S}(\boldsymbol{x})\boldsymbol{y} = \boldsymbol{x} \times \boldsymbol{y}$, where $\boldsymbol{S}(\bullet)$ is a skew-symmetric matrix

$$\boldsymbol{S}(\boldsymbol{x}) = \begin{bmatrix} 0 & -x_3 & x_2 \\ x_3 & 0 & -x_1 \\ -x_2 & x_1 & 0 \end{bmatrix} \tag{1}$$

which gives $\boldsymbol{S}(\bullet) = -\boldsymbol{S}(\bullet)^\top, \boldsymbol{x}^\top\boldsymbol{S}(\bullet)\boldsymbol{x} = 0,\ \boldsymbol{x}^\top\boldsymbol{S}(\boldsymbol{x}) = \boldsymbol{0},\ \forall \boldsymbol{x}, \boldsymbol{S}(\boldsymbol{x})\boldsymbol{y} = -\boldsymbol{S}(\boldsymbol{y})\boldsymbol{x}$. Moreover the cross-product gives the difference in angle-axis between two vectors

$$\boldsymbol{S}(\boldsymbol{x})\boldsymbol{y} = \|\boldsymbol{x}\|\|\boldsymbol{y}\| \sin(\theta)\boldsymbol{u} \tag{2}$$

where θ is the angle between the vectors, and $\boldsymbol{u}$ is the axis of the rotation, which is orthogonal to the two vectors. The dynamics of a rotation matrix $\boldsymbol{\mathcal{R}}_{nb}$, from body b to inertia frame n, is described by

$$\dot{\boldsymbol{\mathcal{R}}}_{nb} = \boldsymbol{\mathcal{R}}_{nb}\boldsymbol{S}(\boldsymbol{\omega}) \tag{3}$$

where $\boldsymbol{\omega} = \boldsymbol{\omega}_{nb}^b$ is the angular velocity of the frame b relative to n decomposed in b.

B. Unit Vector Dynamics

Directional measurements of a vector $\boldsymbol{x}$ can be provided as a unit vector $\boldsymbol{u}_x = \frac{\boldsymbol{x}}{\|\boldsymbol{x}\|}$. This can be for instance the bearing vector to a landmark or a velocity direction from a camera. These measurements can be measured in the inertial-frame $\boldsymbol{u}_x^n$ or body frame $\boldsymbol{u}_x^b$. The real vector corresponding to the directional measurement will have a magnitude, and a time derivative in the inertial-frame

$$z = \|\boldsymbol{x}^n\| \qquad \dot{\boldsymbol{x}}^n = \boldsymbol{w}_x^n \tag{4}$$

The derivative can correspond to the velocity of the vehicle, if the vector is a distance vector from the vessel to a stationary point. Alternatively, it can correspond to acceleration, if the vector is inertial velocity.

By combining (3) and (4) we can get the dynamic of the vector magnitude and unit vector in inertial- and body-frame, visualized in Figure 1,

$$z^2 = (\boldsymbol{x})^\top\boldsymbol{x} \tag{5}$$

$$2z\dot{z} = 2(\boldsymbol{x})^\top\dot{\boldsymbol{x}} \tag{6}$$

$$\dot{z} = (\boldsymbol{u}_x^n)^\top\boldsymbol{w}_x^n = (\boldsymbol{u}_x^b)^\top\boldsymbol{w}_x^b \tag{7}$$

These results will then be used for deriving the dynamics of the unit vector

$$\dot{\boldsymbol{u}}_x^n = \frac{\dot{\boldsymbol{x}}^n}{z} - \frac{\boldsymbol{x}^n}{z^2}\dot{z} = \frac{\boldsymbol{w}_x^n}{z} - \frac{\boldsymbol{u}_x^n}{z}(\boldsymbol{u}_x^n)^\top\boldsymbol{w}_x^n \tag{8}$$

$$= \frac{1}{z}(\boldsymbol{I} - \boldsymbol{u}_x^n(\boldsymbol{u}_x^n)^\top)\boldsymbol{w}_x^n \tag{9}$$

$$\dot{\boldsymbol{u}}_x^n = -\frac{1}{z}S(\boldsymbol{u}_x^n)^2\boldsymbol{w}_x^n \tag{10}$$

where it is clear that the unit vector will be maintained on the unit sphere since $(\boldsymbol{u}_x^n)^\top\dot{\boldsymbol{u}}_x^n = 0$. For the dynamics of the unit vector in body coordinates we need to take into account the rotation of the body coordinate frame

$$\boldsymbol{x}^b = (\boldsymbol{\mathcal{R}}_{nb})^\top\boldsymbol{x}^n \tag{11}$$

$$\Downarrow$$

$$\dot{\boldsymbol{x}}^b = -S(\boldsymbol{\omega})\boldsymbol{x}^b + \boldsymbol{w}_x^b \tag{12}$$

which gives the unit vector dynamics

$$\dot{\boldsymbol{u}}_x^b = \frac{\dot{\boldsymbol{x}}^b}{z} - \frac{\boldsymbol{x}^b}{z^2}\dot{z} \tag{13}$$

$$= \frac{-S(\boldsymbol{\omega})\boldsymbol{x}^b + \boldsymbol{w}_x^b}{z} - \frac{\boldsymbol{x}^b}{z^2}(\boldsymbol{u}_x^b)^\top\boldsymbol{w}_x^b \tag{14}$$

$$= -S(\boldsymbol{\omega})\boldsymbol{u}_x^b + \frac{1}{z}(\boldsymbol{I} - \boldsymbol{u}_x^b(\boldsymbol{u}_x^b)^\top)\boldsymbol{w}_x^b \tag{15}$$

$$= -S(\boldsymbol{\omega})\boldsymbol{u}_x^b - \frac{1}{z}S(\boldsymbol{u}_x^b)^2\boldsymbol{w}_x^b \tag{16}$$

This unit vector is also maintained on the unit sphere by the same argument. The inverted magnitude $d = \frac{1}{z}$ will have the dynamic

$$\dot{d} = d^2(\boldsymbol{u}_x^n)^\top\boldsymbol{w}_x^n = d^2(\boldsymbol{u}_x^b)^\top\boldsymbol{w}_x^b \tag{17}$$

III. Vector Magnitude Observer

The main goal of the observer is to estimate the magnitude of a vector, given that its unit vector (direction) is measured together with the time derivative of the vector. The observer using measurements in the inertial frame is

$$\dot{\hat{\boldsymbol{u}}}_x^n = -\boldsymbol{S}(k\boldsymbol{\sigma})\hat{\boldsymbol{u}}_x^n - \hat{d}\boldsymbol{S}(\hat{\boldsymbol{u}}_x^n)\boldsymbol{S}(\boldsymbol{u}_x^n)\boldsymbol{w}_x^n \tag{18}$$

$$\dot{\hat{d}} = \text{Proj}_d(-\gamma(\boldsymbol{w}_x^n)^\top\boldsymbol{S}(\boldsymbol{u}_x^n)^2\boldsymbol{S}(\hat{\boldsymbol{u}}_x^n)\boldsymbol{\sigma}) + \text{Proj}_d(\hat{d}^2(\boldsymbol{u}_x^n)^\top\boldsymbol{w}_x^n))$$

$$\boldsymbol{\sigma} = \boldsymbol{S}(\boldsymbol{u}_x^n)\hat{\boldsymbol{u}}_x^n \tag{19}$$

where $\boldsymbol{u}_x^n$ is the unit vector measurement with corresponding estimate $\hat{\boldsymbol{u}}_x^n$; the input $\boldsymbol{w}_x^n$ is the vector derivative; the estimate $\hat{d}$ is the estimate of the *unknown* inverted magnitude d; k and γ are positive tuning parameters. $\text{Proj}_d(\bullet)$ is the projection operator from [12, Lemma E.1] working as a continuous saturation ensuring $\underline{d} < \hat{d} < \bar{d}$. All the functions and inputs are continuous in all parameters and locally Lipschitz so that a unique solution is guaranteed. We note that the estimate $\hat{\boldsymbol{u}}_x^n$ will be maintained on the unit sphere if it starts on the unit sphere, since $(\hat{\boldsymbol{u}}_x^n)^\top\dot{\hat{\boldsymbol{u}}}_x^n = 0$. We continue

by investigating the error dynamics of the observer, defined by the error variables $\tilde{\boldsymbol{u}}_x^n = \boldsymbol{S}(\boldsymbol{u}_x^n)\hat{\boldsymbol{u}}_x^n, \quad \tilde{d} = d - \hat{d}$

$$\dot{\tilde{\boldsymbol{u}}}_x^n = \boldsymbol{S}(\boldsymbol{u}_x^n)\dot{\hat{\boldsymbol{u}}}_x^n - \boldsymbol{S}(\hat{\boldsymbol{u}}_x^n)\dot{\boldsymbol{u}}_x^n \tag{20}$$

$$\begin{aligned}=&\boldsymbol{S}(\boldsymbol{u}_x^n)(-\boldsymbol{S}(k\boldsymbol{\sigma})\hat{\boldsymbol{u}}_x^n - \hat{d}\boldsymbol{S}(\hat{\boldsymbol{u}}_x^n)\boldsymbol{S}(\boldsymbol{u}_x^n)\boldsymbol{w}_x^n)\\ &+ d\boldsymbol{S}(\hat{\boldsymbol{u}}_x^n)\boldsymbol{S}(\boldsymbol{u}_x^n)^2\boldsymbol{w}_x^n\end{aligned} \tag{21}$$

$$\begin{aligned}=&k\boldsymbol{S}(\boldsymbol{u}_x^n)\boldsymbol{S}(\hat{\boldsymbol{u}}_x^n)\tilde{\boldsymbol{u}}_x^n - \hat{d}\boldsymbol{S}(\boldsymbol{u}_x^n)\boldsymbol{S}(\hat{\boldsymbol{u}}_x^n)\boldsymbol{S}(\boldsymbol{u}_x^n)\boldsymbol{w}_x^n\\ &+ (\tilde{d} + \hat{d})\boldsymbol{S}(\hat{\boldsymbol{u}}_x^n)\boldsymbol{S}(\boldsymbol{u}_x^n)\boldsymbol{S}(\boldsymbol{u}_x^n)\boldsymbol{w}_x^n\end{aligned} \tag{22}$$

$$\begin{aligned}=&k\boldsymbol{S}(\boldsymbol{u}_x^n)\boldsymbol{S}(\hat{\boldsymbol{u}}_x^n)\tilde{\boldsymbol{u}}_x^n + \tilde{d}\boldsymbol{S}(\hat{\boldsymbol{u}}_x^n)\boldsymbol{S}(\boldsymbol{u}_x^n)\boldsymbol{S}(\boldsymbol{u}_x^n)\boldsymbol{w}_x^n\\ &+ \hat{d}\boldsymbol{S}(\boldsymbol{S}(\boldsymbol{u}_x^n)\boldsymbol{w}_x^n)\tilde{\boldsymbol{u}}_x^n\end{aligned} \tag{23}$$

where we note that $\boldsymbol{S}(\boldsymbol{u}_x^n)\boldsymbol{S}(\hat{\boldsymbol{u}}_x^n) - \boldsymbol{S}(\hat{\boldsymbol{u}}_x^n)\boldsymbol{S}(\boldsymbol{u}_x^n) = \boldsymbol{S}(\tilde{\boldsymbol{u}}_x^n)$ is utilized. We then get the following expression for the error dynamics

$$\begin{aligned}\dot{\tilde{\boldsymbol{u}}}_x^n =& k\boldsymbol{S}(\boldsymbol{u}_x^n)\boldsymbol{S}(\hat{\boldsymbol{u}}_x^n)\tilde{\boldsymbol{u}}_x^n + \hat{d}\boldsymbol{S}(\boldsymbol{S}(\boldsymbol{u}_x^n)\boldsymbol{w}_x^n)\tilde{\boldsymbol{u}}_x^n\\ &+ \boldsymbol{S}(\hat{\boldsymbol{u}}_x^n)\boldsymbol{S}(\boldsymbol{u}_x^n)\boldsymbol{S}(\boldsymbol{u}_x^n)\boldsymbol{w}_x^n\tilde{d}\end{aligned} \tag{24}$$

$$\begin{aligned}\dot{\tilde{d}} =& d^2(\boldsymbol{u}_x^n)^\top\boldsymbol{w}_x^n\\ &- \text{Proj}_d(-\gamma(\boldsymbol{w}_x^n)^\top\boldsymbol{S}(\boldsymbol{u}_x^n)\boldsymbol{S}(\boldsymbol{u}_x^n)\boldsymbol{S}(\hat{\boldsymbol{u}}_x^n)\tilde{\boldsymbol{u}}_x^n)\\ &- \text{Proj}_d(\hat{d}^2(\boldsymbol{u}_x^n)^\top\boldsymbol{w}_x^n)\end{aligned} \tag{25}$$

We will also use the the angle error $\tilde{\theta}$ between $\boldsymbol{u}_x^n$ and $\hat{\boldsymbol{u}}_x^n$, with $\|\tilde{\boldsymbol{u}}_x^n\| = \sin(\tilde{\theta})$ and $(\boldsymbol{u}_x^n)^\top\hat{\boldsymbol{u}}_x^n = \cos(\tilde{\theta})$.

For the guaranteed stability of the observers error dynamic, we need the unit vector derivative and the vector magnitude to be non zero, this will ensure that the system is persistently excited

Lemma 1: Consider the function

$$\mathcal{B}_u(t) = \mathcal{B}(t, \boldsymbol{u}_x^n, \hat{\boldsymbol{u}}_x^n, \boldsymbol{w}_x^n) = \boldsymbol{S}(\hat{\boldsymbol{u}}_x^n)\boldsymbol{S}(\boldsymbol{u}_x^n)\boldsymbol{S}(\boldsymbol{u}_x^n)\boldsymbol{w}_x^n \tag{26}$$

representing the skew-symmetric part of the error dynamics (24)-(25). If there exist a constant $\underline{u}$ such that $\|\dot{\boldsymbol{u}}_x^n\| \geq \underline{u} > 0$ and the magnitude of the vector satisfies $z > \underline{z} > 0$ and there is an ϵ so that $(\hat{\boldsymbol{u}}_x^n)^\top\boldsymbol{u}_x^n > \cos(\epsilon)$, then there exists a $\mu > 0$ so that

$$\mathcal{B}_u(t)^\top\mathcal{B}_u(t) > \mu \tag{27}$$

Proof: If we substitute (10) into (26), we get

$$\mathcal{B}_u(t) = z\boldsymbol{S}(\hat{\boldsymbol{u}}_x^n)\dot{\boldsymbol{u}}_x^n \tag{28}$$

We know that $\dot{\boldsymbol{u}}_x^n$ is orthogonal to $\boldsymbol{u}_x^n$ and will therefore not be parallel to $\hat{\boldsymbol{u}}_x^n$. Using (2) we see that the norm $\|\mathcal{B}_u(t)\|$ will be bounded from below as long as $\|\dot{\boldsymbol{u}}_x^n\|$ and z are bounded from below

$$\mathcal{B}_u(t)^\top\mathcal{B}_u(t) \geq \cos\epsilon^2\underline{z}^2\underline{u}^2 > \mu \tag{29}$$

■

More specific assumptions on the system are

- A1 The vector measurement is so that the constants from Lemma 1 $\|\dot{\boldsymbol{u}}_x^n\| \geq \underline{u}$, $z > \underline{z}(d < \bar{d})$ exists. The input derivative is also bounded from above $\|\boldsymbol{w}_x^n\| < \bar{w}$.
- A2 There exist an arbitrary small angle $0 < \epsilon < \pi$, and the tuning parameters γ and k are chosen to satisfy

$$k > \max(\frac{\bar{d}\bar{w}}{\sin(\epsilon)}, \frac{4\bar{w}^3\bar{d}}{\cos(\epsilon)}, \frac{\bar{w}^2\bar{d}}{\mu} - \frac{\bar{\rho}_\delta}{\bar{w}}, \frac{2\bar{w}^3\bar{d}^2}{\check{d}\mu}) \tag{30}$$

$$\frac{\bar{w}^3\bar{d}}{(k\bar{w} + \bar{\rho}_\delta)^2} < \delta < \min(\frac{\mu}{4\bar{w}^3\bar{d}}, \frac{k\cos(\epsilon)\mu}{4(k\bar{w} + \bar{\rho}_\delta)^2}) \tag{31}$$

$$\frac{2\bar{d}\bar{w}}{\mu\delta} < \gamma < \min(\frac{1}{\bar{w}^2\delta^2}, \frac{2(k\bar{w} + \bar{\rho}_\delta)^2}{\bar{w}^2\mu}) \tag{32}$$

where the details of the constants δ, ϵ, $\check{d}$ and $\bar{\rho}_\delta$ are seen in the proof of Theorem 1.

Theorem 1: Consider the vector $\boldsymbol{x}^n$ with the *unknown* time varying magnitude $z = \frac{1}{d}$. Assume its unit vector $\boldsymbol{u}_x^n = \frac{\boldsymbol{x}^n}{\|\boldsymbol{x}^n\|}$ is measured together with its derivative vector $\dot{\boldsymbol{x}}^n = \boldsymbol{w}_x^n$, and the assumptions A1-A2 holds. Then the error dynamics of the observer (18)-(19) will be UAS for every initial condition satisfying $(\hat{\boldsymbol{u}}_x^n)^\top\boldsymbol{u}_x^n > -\cos(\epsilon)$, $\hat{d} \leq \bar{d}$ and UES for $\underline{d} \leq \hat{d} \leq \bar{d}$ and $(\hat{\boldsymbol{u}}_x^n)^\top\boldsymbol{u}_x^n > \cos(\epsilon)$, so that the errors $(\hat{\boldsymbol{u}}_x^n)^\top\boldsymbol{u}_x^n \to 1$, $\tilde{\boldsymbol{u}}_x^n = \boldsymbol{S}(\boldsymbol{u}_x^n)\hat{\boldsymbol{u}}_x^n \to \boldsymbol{0}$ and $\tilde{d} = d - \hat{d} \to 0$ as $t \to \infty$

The proof will be structured in the following way:

Outline of the proof:

- A) First prove that the the errors of the observer (18)-(19) is bounded so the angular error $\tilde{\theta}$ between $\boldsymbol{u}_x^n$ and $\hat{\boldsymbol{u}}_x^n$ is bounded away from $|\tilde{\theta}| < \pi - \epsilon$ and converges in finite time to the set $|\tilde{\theta}| \leq \epsilon$.
- B) Define a Lyapunov function candidate and its derivative
- C) Utilise the conditions and bounds from the assumptions, and prove that the Lyapunov function candidate derivative is negative definite in the set $|\tilde{\theta}| \leq \epsilon$ found in A)
- D) Verify that it is maintained negative definite when projection is activated.

Proof:

A): We know that the estimate $\hat{d}$ is bounded by the projection, and we have assumed that $d < \bar{d}$ since $z > \underline{z}$, which means the $\tilde{d}$ is also bounded. To obtain the boundedness of the error $\tilde{\theta}$ we use the Lyapunov-like function

$$V_1 = 1 - (\boldsymbol{u}_x^n)^\top\hat{\boldsymbol{u}}_x^n = 1 - cos(\tilde{\theta}) \tag{33}$$

which is clearly positive definite for $0 < |\tilde{\theta}| < \pi$. Its derivative is

$$\dot{V}_1 = -(\dot{\boldsymbol{u}}_x^n)^\top\hat{\boldsymbol{u}}_x^n - (\boldsymbol{u}_x^n)^\top\dot{\hat{\boldsymbol{u}}}_x^n \tag{34}$$

$$\begin{aligned}=&-(d\boldsymbol{S}(\boldsymbol{u}_x^n)^2\boldsymbol{w}_x^n)^\top\hat{\boldsymbol{u}}_x^n\cdots\\ &- (\boldsymbol{u}_x^n)^\top(-\boldsymbol{S}(k\boldsymbol{\sigma})\hat{\boldsymbol{u}}_x^n + \hat{d}\boldsymbol{S}(\hat{\boldsymbol{u}}_x^n)\boldsymbol{S}(\boldsymbol{u}_x^n)\boldsymbol{w}_x^n)\end{aligned} \tag{35}$$

$$= (\boldsymbol{u}_x^n)^\top\boldsymbol{S}(k\boldsymbol{\sigma})\hat{\boldsymbol{u}}_x^n + \tilde{d}(\boldsymbol{u}_x^n)^\top(\boldsymbol{S}(\hat{\boldsymbol{u}}_x^n)\boldsymbol{S}(\boldsymbol{u}_x^n)\boldsymbol{w}_x^n) \tag{36}$$

$$= -k\|\tilde{\boldsymbol{u}}_x^n\|^2 + \tilde{d}(\tilde{\boldsymbol{u}}_x^n)^\top\boldsymbol{S}(\boldsymbol{u}_x^n)\boldsymbol{w}_x^n \tag{37}$$

$$\leq -\|\tilde{\boldsymbol{u}}_x^n\|(k\|\tilde{\boldsymbol{u}}_x^n\| - \bar{d}\bar{w}) \tag{38}$$

We know that $\tilde{\theta} = \pi - \epsilon$ corresponds to an error $\|\tilde{\boldsymbol{u}}_x^n\| = \sin(\epsilon)$. So for any arbitary small $\epsilon > 0$ there exists $\underline{k} > \frac{\bar{d}\bar{w}}{\sin(\epsilon)}$ so that any $k \geq \underline{k}$ will ensure that $\dot{V}_1 < 0$; hence we can conclude that the error is bounded away from $\tilde{\theta} = \pm\pi$ and that the unit vector estimate will converge to the set $|\tilde{\theta}| \leq \epsilon$ in finite time [13, Theorem 3.18]. From here we will use that this bound holds, which implies that $\|\tilde{\boldsymbol{u}}_x^n\| < 1 \Leftrightarrow |\tilde{\theta}| < \frac{\pi}{2}$,

and $\|\tilde{\boldsymbol{u}}_x^n\| = 0 \Leftrightarrow |\tilde{\theta}| = 0$. We will then show that the system is UES when $|\tilde{\theta}| \leq \epsilon$.

B): We choose the Lyapunov function candidate

$$V_2(t, \tilde{\boldsymbol{u}}_x^n, \tilde{d}) = \frac{1}{2}(\tilde{\boldsymbol{u}}_x^n)^\top(\tilde{\boldsymbol{u}}_x^n) + \frac{1}{2\gamma}\tilde{d}^2 - \delta(\tilde{\boldsymbol{u}}_x^n)^\top \mathcal{B}_u(t)\tilde{d} \tag{39}$$

with $\delta > 0$. To ensure that the Lyapunov function candidate is positive definite, we impose the constraint $\delta^2 < \frac{1}{\gamma\bar{w}^2}$ since we know that $\bar{w} \geq \|\mathcal{B}_u(t)\|$ by Assumption A1. If we then take the time-derivative along the trajectory of the error dynamics (24)-(25) we get

$$\begin{aligned}
\dot{V}_2 = \; & (\tilde{\boldsymbol{u}}_x^n)^\top(k\boldsymbol{S}(\boldsymbol{u}_x^n)\boldsymbol{S}(\hat{\boldsymbol{u}}_x^n)\tilde{\boldsymbol{u}}_x^n + \hat{d}\boldsymbol{S}(\boldsymbol{S}(\boldsymbol{u}_x^n)\boldsymbol{w}_x^n)\tilde{\boldsymbol{u}}_x^n) \\
& + (\tilde{\boldsymbol{u}}_x^n)^\top \mathcal{B}_u(t)\tilde{d} + \frac{1}{\gamma}\tilde{d}d^2(\boldsymbol{u}_x^n)^\top \boldsymbol{w}_x^n \\
& - \frac{1}{\gamma}\tilde{d}\text{Proj}_d(\hat{d}^2(\boldsymbol{u}_x^n)^\top \boldsymbol{w}_x^n) - \frac{1}{\gamma}\tilde{d}\text{Proj}_d(\gamma\mathcal{B}_u(t)^\top \tilde{\boldsymbol{u}}_x^n)) \\
& - \delta\tilde{\boldsymbol{u}}_x^n\dot{\mathcal{B}}_u(t)\tilde{d} - \delta\tilde{d}\mathcal{B}_u(t)^\top \mathcal{B}_u(t)\tilde{d} \\
& + \delta\hat{d}(\tilde{\boldsymbol{u}}_x^n)^\top \boldsymbol{S}(\boldsymbol{S}(\boldsymbol{u}_x^n)\boldsymbol{w}_x^n)\mathcal{B}_u(t)\tilde{d} \\
& + \delta k((\boldsymbol{u}_x^n)^\top \hat{\boldsymbol{u}}_x^n)(\tilde{\boldsymbol{u}}_x^n)^\top \mathcal{B}_u(t)\tilde{d} \\
& - \delta(\tilde{\boldsymbol{u}}_x^n)^\top \mathcal{B}_u(t)d^2(\boldsymbol{u}_x^n)^\top \boldsymbol{w}_x^n \\
& + \delta(\tilde{\boldsymbol{u}}_x^n)^\top \mathcal{B}_u(t)(\text{Proj}_d(\hat{d}^2(\boldsymbol{u}_x^n)^\top \boldsymbol{w}_x^n) + \text{Proj}_d(\gamma\mathcal{B}_u(t)^\top \tilde{\boldsymbol{u}}_x^n))
\end{aligned} \tag{40}$$

where we use the vector product to get $\boldsymbol{S}(\boldsymbol{u}_x^n)\boldsymbol{S}(\hat{\boldsymbol{u}}_x^n)\tilde{\boldsymbol{u}}_x^n = -((\boldsymbol{u}_x^n)^\top \hat{\boldsymbol{u}}_x^n)\tilde{\boldsymbol{u}}_x^n$,

C): First we assume that projection is not being activated. We use the bounds in the assumption A1, where there exists positive constants $\bar{\rho}_2 = \bar{w}$, $\bar{\rho}_4 = 2\bar{d}\bar{w}$ and $\bar{\rho}_5 = \bar{d}\bar{w}$. From the Lipschitz property a constant $\bar{b}_d > \|\dot{\mathcal{B}}_u(t)\|$ exist, and from the boundedness from paragraph A) there is a maximum angle ϵ between $\boldsymbol{u}_x^n$ and $\hat{\boldsymbol{u}}_x^n$ so that $k_\epsilon = k\cos(\epsilon) < k(\hat{\boldsymbol{u}}_x^n)^\top \boldsymbol{u}_x^n$. In addition, the ϵ combined with the assumptions in A1 guarantee that Lemma 1 will hold, hence we can use (27). With these bounds we can rearrange $\dot{V}_2$ to the inequality

$$\begin{aligned}
\dot{V}_2 \leq \; & -k_\epsilon\|\tilde{\boldsymbol{u}}_x^n\|^2 + \delta\gamma\bar{\rho}_2^2\|\tilde{\boldsymbol{u}}_x^n\|^2 - \delta\mu\tilde{d}^2 + \frac{1}{\gamma}\tilde{d}^2\bar{\rho}_4 \\
& + \delta\bar{b}_d\|\tilde{\boldsymbol{u}}_x^n\|\tilde{d} + \delta\|\tilde{\boldsymbol{u}}_x^n\|\tilde{d}\bar{\rho}_2(\bar{\rho}_4 + \bar{\rho}_5) \\
& (-k(\boldsymbol{u}_x^n)^\top \hat{\boldsymbol{u}}_x^n + (\frac{1}{2} - \frac{1}{2})(\min(k_\epsilon, \delta\mu\gamma))\delta(\tilde{\boldsymbol{u}}_x^n)^\top \mathcal{B}_u(t)\tilde{d}
\end{aligned}$$

where the last zero term is added to easier see the exponential result, and by using $k > k(\boldsymbol{u}_x^n)^\top \hat{\boldsymbol{u}}_x^n - \frac{1}{2}\min(k_\epsilon, \delta\mu\gamma)$, the inequality can be reorganized to

$$\begin{aligned}
\dot{V}_2 < & -\|\tilde{\boldsymbol{u}}_x^n\|^2\frac{k_\epsilon}{4} - \tilde{d}^2\frac{\delta\mu}{4} \\
& + \frac{1}{2}\min(k_\epsilon, \delta\mu\gamma)\delta(\tilde{\boldsymbol{u}}_x^n)^\top \mathcal{B}_u(t)\tilde{d} \\
& - \|\tilde{\boldsymbol{u}}_x^n\|^2(\frac{k_\epsilon}{2} - \delta\gamma\bar{\rho}_2^2) - \tilde{d}^2(\frac{\delta\mu}{2} - \frac{\bar{\rho}_4}{\gamma}) \\
& -\frac{1}{2}\begin{bmatrix}\|\tilde{\boldsymbol{u}}_x^n\| \\ \tilde{d}\end{bmatrix}^\top \begin{bmatrix}\frac{k_\epsilon}{2} & -\delta(k\bar{\rho}_2 + \bar{\rho}_\delta) \\ -\delta(k\bar{\rho}_2 + \bar{\rho}_\delta) & \frac{\delta\mu}{2}\end{bmatrix}\begin{bmatrix}\|\tilde{\boldsymbol{u}}_x^n\| \\ \tilde{d}\end{bmatrix}
\end{aligned} \tag{41, 42}$$

where $\bar{\rho}_\delta = \bar{b}_d + \bar{\rho}_2(\bar{\rho}_4 + \bar{\rho}_5)$. We see that we need the variables and tuning parameters to satisfy the following inequalities,

$$k > \max(\frac{\bar{d}\bar{w}}{\sin(\epsilon)}, \frac{2\delta\gamma\bar{\rho}_2^2}{\cos(\epsilon)}) \tag{43}$$

$$\delta^2 < \frac{1}{\gamma\bar{\rho}_2^2}, \; \frac{2\bar{\rho}_4}{\gamma\mu} < \delta < \frac{k\cos(\epsilon)\mu}{4(k\bar{\rho}_2 + \bar{\rho}_\delta)^2} \tag{44}$$

to ensure that $\dot{V}_2 \leq -\frac{1}{2}\min(k_\epsilon, \delta\mu\gamma)V_2$. We can reorganize the inequaleties

$$k > \max(\frac{\bar{d}\bar{w}}{\sin(\epsilon)}, \frac{2\bar{\rho}_2^2\bar{\rho}_4}{\mu\cos(\epsilon)}, \frac{\bar{\rho}_2\bar{\rho}_4}{\mu} - \frac{\bar{\rho}_\delta}{\bar{\rho}_2}) \tag{45}$$

$$\frac{2\bar{\rho}_2^2\bar{\rho}_4}{4(k\bar{\rho}_2 + \bar{\rho}_\delta)^2} < \delta < \min(\frac{k\cos(\epsilon)\mu}{4(k\bar{\rho}_2 + \bar{\rho}_\delta)^2}, \frac{\mu}{2\bar{\rho}_2^2\bar{\rho}_4}) \tag{46}$$

$$\frac{2\bar{\rho}_4}{\mu\delta} < \gamma < \min(\frac{1}{\delta^2\bar{\rho}_2^2}, \frac{2(k\bar{\rho}_2 + \bar{\rho}_\delta)^2}{\mu\bar{\rho}_2^2}) \tag{47}$$

by substituting the $\bar{\rho}_\bullet$ with their corresponding bounds, we see that this will hold by assumption A2. Hence, we can conclude that δ and γ can be choosen if k is high enough so that the system is uniformly exponentially stable when the projection is not activated, and it will have converges rate of $\frac{1}{2}\min(k_\epsilon, \delta\mu\gamma)$.

D): There are four projections in (40). By using

$$\begin{aligned}
-\boldsymbol{y}^\top\boldsymbol{\Gamma}^{-1}\text{Proj}_y(\tau) &\leq -\boldsymbol{y}^\top\boldsymbol{\Gamma}^{-1}(\tau) \\
\|\text{Proj}_y(\tau)\| &< \|\tau\|
\end{aligned}$$

from [12, E.1], three of the terms can be handled trivially.

$$-\frac{1}{\gamma}\tilde{d}\text{Proj}_d(\hat{d}^2(\boldsymbol{u}_x^n)^\top \boldsymbol{w}_x^n) < -\frac{1}{\gamma}\tilde{d}\hat{d}^2(\boldsymbol{u}_x^n)^\top \boldsymbol{w}_x^n \tag{48}$$

$$-\frac{1}{\gamma}\tilde{d}\text{Proj}_d(\gamma\mathcal{B}_u(t)^\top \tilde{\boldsymbol{u}}_x^n)) < -\frac{1}{\gamma}\tilde{d}\gamma\mathcal{B}_u(t)^\top \tilde{\boldsymbol{u}}_x^n \tag{49}$$

$$\|\delta(\tilde{\boldsymbol{u}}_x^n)^\top \mathcal{B}_u(t)\text{Proj}_d(\gamma\mathcal{B}_u(t)^\top \tilde{\boldsymbol{u}}_x^n)\| < \tag{50}$$

$$\|\delta(\tilde{\boldsymbol{u}}_x^n)^\top \mathcal{B}_u(t)\gamma\mathcal{B}_u(t)^\top \tilde{\boldsymbol{u}}_x^n\| \tag{51}$$

Which gives the same inequality terms as in (42). The fourth projection term is

$$\delta(\tilde{\boldsymbol{u}}_x^n)^\top \mathcal{B}_u(t)\text{Proj}_d(\hat{d}^2(\boldsymbol{u}_x^n)^\top \boldsymbol{w}_x^n) \tag{52}$$

which cancels out term

$$-\delta(\tilde{\boldsymbol{u}}_x^n)^\top \mathcal{B}_u(t)d^2(\boldsymbol{u}_x^n)^\top \boldsymbol{w}_x^n \tag{53}$$

when the projection is not activated; utilizing $(d^2 - \hat{d}^2) < 2\tilde{d}\bar{d}$. When the projection (52) is activated, the projection term becomes zero, meaning that another term is needed to handle (53). However, since the projection (52) is activated, it implies that $\tilde{d}\hat{d}^2(\boldsymbol{u}_x^n)^\top \boldsymbol{w}_x^n < 0 \Leftrightarrow \frac{1}{\gamma}\tilde{d}d^2(\boldsymbol{u}_x^n)^\top \boldsymbol{w}_x^n < 0$, which is available as the projection counter part (48) is zero, since it is also activated. This term can therefore be used against (53), meaning that if the inequality

$$\|\frac{1}{\gamma}\tilde{d}\hat{d}^2(\boldsymbol{u}_x^n)^\top \boldsymbol{w}_x^n\| > \|\delta(\tilde{\boldsymbol{u}}_x^n)^\top \mathcal{B}_u(t)d^2(\boldsymbol{u}_x^n)^\top \boldsymbol{w}_x^n\| \tag{54}$$

holds, inequality (42) will also hold when the projection is activated. By utilizing that the $\tilde{d}$ is non zero as the projection is activated, and the bound $\tilde{\boldsymbol{u}}_x^n < \sin(\epsilon)$ we see that this inequality is equivalent to

$$\sin(\epsilon) < \frac{|\tilde{d}|}{\gamma\delta\bar{\rho}_2} \Rightarrow k > \frac{2\bar{w}^3\bar{d}^2}{\check{d}\mu} \tag{55}$$

where $\check{d}$ is the minimum error $|\tilde{d}|$ can be while the projection is activated. Thus we see that the derivative of the Lyapunov function candidate is maintained negative definite while the projection is activated. Proving that the observer converges to zero exponentially fast when $|\tilde{\theta}| \leq \epsilon$. In addition, we proved in A) that the error will converge to this set $|\tilde{\theta}| \leq \epsilon$ in finite time, so combining these results the observer is UAS for the error dynamics for all initial conditions according to Theorem 1, and and UES when $|\tilde{\theta}| \leq \epsilon$. ■

From the proof we see that the region of attraction for the observer is determined by a parameter ϵ, which can be arbitrary small while increasing k, so the stability is in practice semi-global on the sphere. From the proof we also see that the exponential convergence rate is $\frac{1}{2}\min(k_\epsilon, \delta\mu\gamma)$, although as can be seen in the proof it is a conservative estimate. We also note that the larger the k is, the smaller δ will be, so k should be set large enough, however, if the k is too large, this can limit the convergence of the $\tilde{d}$. The observer is also be presented in body coordinates, where the difference is the added rotation of the vehicle

$$\dot{\hat{\boldsymbol{u}}}_x^b = -\boldsymbol{S}(\boldsymbol{\omega} + k\boldsymbol{\sigma})\hat{\boldsymbol{u}}_x^b - \hat{d}\boldsymbol{S}(\hat{\boldsymbol{u}}_x^b)\boldsymbol{S}(\boldsymbol{u}_x^b)\boldsymbol{w}_x^b \tag{56}$$

$$\begin{aligned}\dot{\hat{d}} &= \text{Proj}_d(-\gamma(\boldsymbol{w}_x^b)^\top \boldsymbol{S}(\boldsymbol{u}_x^b)^2\boldsymbol{S}(\hat{\boldsymbol{u}}_x^b)\boldsymbol{\sigma}) \\ &\quad + \text{Proj}_d(\hat{d}^2(\boldsymbol{u}_x^b)^\top \boldsymbol{w}_x^b) \\ \boldsymbol{\sigma} &= \boldsymbol{S}(\boldsymbol{u}_x^b)\hat{\boldsymbol{u}}_x^b\end{aligned} \tag{57}$$

Theorem 2: Consider the vector $\boldsymbol{x}^b$ with the *unknown* time varying magnitude $z = \frac{1}{d}$. If the assumptions A1-A2 holds in addition to the angular rate being bounded $\|\boldsymbol{\omega}\| < \bar{\omega}$. Then given the unit vector $\boldsymbol{u}_x^b$ and the derivative $\dot{\boldsymbol{x}}^b = \boldsymbol{w}_x^b$, the error dynamics of the observer (56)-(57) will be UAS for every initial condition satisfying $(\hat{\boldsymbol{u}}_x^b)^\top \boldsymbol{u}_x^b > -\cos(\epsilon)$, $\hat{d} \leq \bar{d}$ and UES for $\underline{d} < \hat{d} < \bar{d}$ and $(\hat{\boldsymbol{u}}_x^b)^\top \boldsymbol{u}_x^b > \cos(\epsilon)$, so that the errors $(\hat{\boldsymbol{u}}_x^b)^\top \boldsymbol{u}_x^b \to 1$, $\tilde{\boldsymbol{u}}_x^b = \boldsymbol{S}(\boldsymbol{u}_x^b)\hat{\boldsymbol{u}}_x^b \to \boldsymbol{0}$ and $\tilde{d} = d - \hat{d} \to 0$ as $t \to \infty$

Proof: Bounded error dynamics follows from

$$\dot{V}_1^b = \leq \|\tilde{\boldsymbol{u}}_x^b\|(k\|\tilde{\boldsymbol{u}}_x^b\| - \bar{d}\boldsymbol{w} + \bar{\omega}) \tag{58}$$

The error dynamics are now

$$\begin{aligned}\dot{\tilde{\boldsymbol{u}}}_x^b &= k\boldsymbol{S}(\boldsymbol{u}_x^b)\boldsymbol{S}(\hat{\boldsymbol{u}}_x^b)\tilde{\boldsymbol{u}}_x^b - \hat{d}\boldsymbol{S}(\boldsymbol{S}(\boldsymbol{u}_x^b)\boldsymbol{w}_x^b)\tilde{\boldsymbol{u}}_x^b \\ &\quad - \boldsymbol{S}(\hat{\boldsymbol{u}}_x^b)\boldsymbol{S}(\boldsymbol{u}_x^b)\boldsymbol{S}(\boldsymbol{u}_x^b)\boldsymbol{w}_x^b\tilde{d} + \boldsymbol{S}(\boldsymbol{\omega})\tilde{\boldsymbol{u}}_x^b\end{aligned} \tag{59}$$

$$\dot{\tilde{d}} = d^2(\boldsymbol{u}_x^b)^\top \boldsymbol{w}_x^b \tag{60}$$

$$\begin{aligned}&- \text{Proj}_d(-\gamma(\boldsymbol{w}_x^b)^\top \boldsymbol{S}(\boldsymbol{u}_x^b)\boldsymbol{S}(\boldsymbol{u}_x^b)\boldsymbol{S}(\hat{\boldsymbol{u}}_x^b)\tilde{\boldsymbol{u}}_x^b) \\ &- \text{Proj}_d(\hat{d}^2(\boldsymbol{u}_x^b)^\top \boldsymbol{w}_x^b)\end{aligned} \tag{61}$$

where we see that the difference in error dynamic is the additional skew-symmetric term $\boldsymbol{S}(\boldsymbol{\omega})\tilde{\boldsymbol{u}}_x^b$. We also note that the skew-symmetric part between $\tilde{\boldsymbol{u}}_x^b$ and $\tilde{d}$ is equal to the one from Lemma 1, only that it is in body coordinates, and we know that the norm is preserved by coordinate change, implying that Lemma 1 also applies for the magnitude observer in body coordinates. The only difference of the derivative of V_2^b along this trajectory will be the constant $\bar{\rho}_5 > \boldsymbol{w}\bar{d} + \bar{\omega}$. So similar stability as in Theorem 1 can be concluded for the system (56)-(57), with straight forward change to the proof. ■

Cascade

The next result shows that two instances of the observer can be used in cascade, this means that the output of one observer can be the input of the next observer. One motivation for this can be seen in bearing only SLAM. The first observer is then used to estimate the velocity vector; this vector can then be considered the input of a second observer used for estimating the distance to a landmark.

Theorem 3: Consider two vectors $\boldsymbol{x}_1$ and $\boldsymbol{x}_2$, with corresponding derivatives $\boldsymbol{w}_{x1}$ and $\boldsymbol{w}_{x2}$. Assume directional vectors $\boldsymbol{u}_{x1}$, $\boldsymbol{u}_{x2}$ and the derivative $\boldsymbol{w}_{x1}$ are measured, and the first directional vector $\boldsymbol{u}_{x1} = \frac{\boldsymbol{w}_{x2}}{\|\boldsymbol{w}_{x2}\|}$. Let two observers either according to Theorem 1 or Theorem 2 be in cascade, where the second observer has the input $\hat{\boldsymbol{w}}_{x2} = \frac{\hat{\boldsymbol{u}}_{x1}}{\hat{d}_1}$. We assume assumptions A1-A2 to be true for both observer, in addition, the gain k in the second observer is chosen large enough, and $\hat{d}_1 > \underline{d}_1$ is bounded from below by the projection in the first observer. Then the error dynamics of the whole system will be UAS for every initial condition satisfying $(\hat{\boldsymbol{u}}_{xi})^\top \boldsymbol{u}_{xi} > -\cos(\epsilon)$ and $\hat{d}_i < \bar{d}_i$ for both observers $i \in \{1, 2\}$.

Proof: From cascade theory [14], [15] we know that two sub-systems in cascade being USGAS combined with whole system being bounded implies the whole system being USGAS. What is crucial is to show that regardless of the error from the first observer in cascade, the error in the second observer has the states bounded in the region of attraction, and will not be destabilized. From Theorem 1 or 2 we know that the first observer in the cascade will output an estimate with bounded errors

$$\tilde{\boldsymbol{w}}_{x2} = \boldsymbol{w}_{x2} - \hat{\boldsymbol{w}}_{x2} \tag{62}$$

with the bound $|\tilde{\boldsymbol{w}}_{x2}| \leq \bar{w} \leq \frac{1}{\underline{d}_1}$. We continue by investigating if the second observer in the cascade is still bounded when exposed to this error. For this proof we investigate the boundedness of the observer in Theorem 1, although similar procedure can be done for an observer in Theorem 2, with similar results. We already know that the inverse magnitude estimate $\hat{d}_2 < \bar{d}_2$ and its error $\tilde{d}_2 < \bar{d}_2$ is bounded by the projection operator. We re-examine the Lyapunov-like function $V_1 = 1 - (\boldsymbol{u}_x^n)^\top \hat{\boldsymbol{u}}_x^n$ which will have the derivative

$$\begin{aligned}\dot{V}_1 &= -(\dot{\boldsymbol{u}}_x^n)^\top \hat{\boldsymbol{u}}_x^n - (\boldsymbol{u}_x^n)^\top \dot{\hat{\boldsymbol{u}}}_x^n \\ &= -(d\boldsymbol{S}(\boldsymbol{u}_x^n)^2\boldsymbol{w}_x^n)^\top \hat{\boldsymbol{u}}_x^n \cdots \\ &\quad - (\boldsymbol{u}_x^n)^\top(-\boldsymbol{S}(k\boldsymbol{\sigma})\hat{\boldsymbol{u}}_x^n + \hat{d}\boldsymbol{S}(\hat{\boldsymbol{u}}_x^n)\boldsymbol{S}(\boldsymbol{u}_x^n)\hat{\boldsymbol{w}}_x^n)\end{aligned}$$

$$
\begin{aligned}
=&(\boldsymbol{u}_x^n)^\top \boldsymbol{S}(k\boldsymbol{\sigma})\hat{\boldsymbol{u}}_x^n + (\boldsymbol{u}_x^n)^\top \boldsymbol{S}(\hat{\boldsymbol{u}}_x^n)\boldsymbol{S}(\boldsymbol{u}_x^n)(d\boldsymbol{w}_x^n - \hat{d}\hat{\boldsymbol{w}}_x^n)\\
=&-k\|\tilde{\boldsymbol{u}}_x^n\|^2 + (\tilde{\boldsymbol{u}}_x^n)^\top \boldsymbol{S}(\boldsymbol{u}_x^n)(\tilde{\boldsymbol{w}}_x^n\tilde{d} + \tilde{\boldsymbol{w}}_x^n\hat{d} + \hat{\boldsymbol{w}}_x^n\hat{d})\\
\leq&-\|\tilde{\boldsymbol{u}}_x^n\|(k\|\tilde{\boldsymbol{u}}_x^n\| - 3\bar{d}\bar{w})
\end{aligned}
$$

and with the same argument as from Theorem 1 we can choose a k so that the unit vector estimates are bounded away from $|\tilde{\theta}| < \pi - \epsilon$, and the ϵ can be chosen arbitrary small by increasing k. Clearly the estimates are maintained in the region of attraction of the observer, resulting in the observer error $\tilde{\boldsymbol{u}}_2^n \to \boldsymbol{0}$ and $\tilde{d}_2 \to 0$ as the error $\tilde{\boldsymbol{w}}_{x2} \to \boldsymbol{0}$ converges to zero. ■

Usually in cascade stabillity, a growth condition [14], [15] is introduced to show that the error from a previous system in a cascade will not push the following system out of its region of attraction. For our system this growth condition is not satisfied for the $\tilde{d}$, but due to the projection on this parameter, the observer will not be destabalized. As for the previous results, since ϵ can be chosen arbitrary small we call this USGAS. However, the *peaking phenomenon* should be in mind [16] [14] when tuning the observer in cascade, meaning the second part should be tuned modestly to avoid unnecessary transient error for the second observer.

IV. Example: bearing-only SLAM

To illustrate how the vector magnitude observer may be used, we apply it to the bearing-only SLAM problem. For an overview of the SLAM problem, the readers are refered to [17], [18] and references therein. For our SLAM problem, we want to estimate the ranges $\varrho_i = \|\boldsymbol{\delta}_i\|$ from the vehicle to different landmarks, where $\boldsymbol{\delta}_i$ are the relative position vectors from the vehicle pose to the different landmarks. We assume that we have line of sight (LOS) measurements $\boldsymbol{u}_{i\delta}^b = \frac{\boldsymbol{\delta}_i^b}{\|\boldsymbol{\delta}_i^b\|}$ from these landmarks, in addition, we assume that measurements from an IMU and an attitude heading reference system (AHRS) [19] is available. The AHRS can potentially also estimate the gyro bias, and be viewed as a cascade into the vector magnitude observer, although the setup we present for velocity estimation will be sensitive to attitude error, hence the attitude error should be small. We see that if the LOS measurements are rotated in the earth-fixed frame

$$
\boldsymbol{u}_{i\delta}^n = \boldsymbol{\mathcal{R}}_{nb}\boldsymbol{u}_{i\delta}^b \tag{63}
$$

the derivative of the corresponding relative position vectors is the velocity in the inertial-frame

$$
\dot{\boldsymbol{\delta}}^n = -\boldsymbol{v}^n \tag{64}
$$

which raises the need of a velocity estimate to use the vector magnitude observer to estimate the different ranges.

We assume that we can measure the normalized velocity $\boldsymbol{u}_v^b = \frac{\boldsymbol{v}^b}{\|\boldsymbol{v}^b\|}$; this being for instance available from a camera using methods from optical flow or using homography [9], essential matrix [2] or visual odometry [20]. To estimate the magnitude $\|\boldsymbol{v}^n\|$, we noticing that we can rotate the vector into the inertial-frame $\boldsymbol{u}_v^n = \boldsymbol{\mathcal{R}}_{nb}\boldsymbol{u}_v^b$. In addition, the derivative of the velocity in the inertial-frame is available through the IMU and AHRS

$$
\dot{\boldsymbol{v}}^n = \boldsymbol{\mathcal{R}}_{nb}\boldsymbol{f}_{IMU}^b - \boldsymbol{g}^n \tag{65}
$$

where $\boldsymbol{f}_{IMU}^b$ is the specific force measurements from the IMU, and $\boldsymbol{g}^n$ is the known gravity vector in inertia frame. Meaning the observer can estimate the velocity. The observer is summarized in the following equations

$$
\begin{aligned}
&\boldsymbol{u}_v^n = \boldsymbol{\mathcal{R}}_{nb}\frac{\boldsymbol{v}^b}{\|\boldsymbol{v}^b\|}, \quad \boldsymbol{w}_v^n = \boldsymbol{\mathcal{R}}_{nb}\boldsymbol{f}_{IMU}^b - \boldsymbol{g}^n, \quad d_v = \frac{1}{\boldsymbol{v}^n}\\
&\dot{\hat{\boldsymbol{u}}}_v^n = -S(k_v\boldsymbol{\sigma}_v)\hat{\boldsymbol{u}}_v^n + \hat{d}_v\boldsymbol{S}(\hat{\boldsymbol{u}}_v^n)\boldsymbol{S}(\boldsymbol{u}_v^n)\boldsymbol{w}_v^n\\
&\dot{\hat{d}}_v = \gamma(\boldsymbol{w}_v^n)^\top \boldsymbol{S}(\boldsymbol{u}_v^n)^2\boldsymbol{S}(\hat{\boldsymbol{u}}_v^n)\boldsymbol{\sigma}_v + \hat{d}_v^2(\boldsymbol{u}_v^n)^\top \boldsymbol{w}_v^n\\
&\boldsymbol{\sigma}_v = \boldsymbol{S}(\boldsymbol{u}_v^n)\hat{\boldsymbol{u}}_v^n, \quad \hat{\boldsymbol{v}}^n = \frac{\hat{\boldsymbol{u}}_v^n}{\hat{d}_v}
\end{aligned} \tag{66}
$$

where we for each landmark with index i have

$$
\begin{aligned}
&\boldsymbol{u}_{\delta i}^n = \boldsymbol{\mathcal{R}}_{nb}\boldsymbol{u}_{i\delta}^b, \quad \hat{\boldsymbol{w}}_\delta^n = -\frac{\hat{\boldsymbol{u}}_v^n}{\hat{d}_v}, \quad d_{\delta i} = \frac{1}{\varrho_i}\\
&\dot{\hat{\boldsymbol{u}}}_{\delta i}^n = -S(k_{\delta i}\boldsymbol{\sigma}_{\delta i})\hat{\boldsymbol{u}}_{\delta i}^n + \hat{d}_{\delta i}\boldsymbol{S}(\hat{\boldsymbol{u}}_{\delta i}^n)\boldsymbol{S}(\boldsymbol{u}_{\delta i}^n)\hat{\boldsymbol{w}}_\delta^n\\
&\dot{\hat{d}}_{\delta i} = \gamma(\hat{\boldsymbol{w}}_\delta^n)^\top \boldsymbol{S}(\boldsymbol{u}_{\delta i}^n)^2\boldsymbol{S}(\hat{\boldsymbol{u}}_{\delta i}^n)\boldsymbol{\sigma}_{\delta i} + \hat{d}_{\delta i}^2(\boldsymbol{u}_{\delta i}^n)^\top \hat{\boldsymbol{w}}_\delta^n\\
&\boldsymbol{\sigma}_{\delta i} = \boldsymbol{S}(\boldsymbol{u}_{\delta i}^n)\hat{\boldsymbol{u}}_{\delta i}^n, \quad \hat{\boldsymbol{\delta}}_i^n = \frac{\hat{\boldsymbol{u}}_{\delta i}^n}{\hat{d}_{\delta i}}
\end{aligned} \tag{67}
$$

The cascade structure of this bearing only SLAM with 4 landmarks can be seen in Figure 2. By the theorems in the previous chapters the error dynamics of this system is USGAS under certain assumptions. One of these assumptions is that the velocity vector is bounded from below, meaning that the USGAS of the velocity magnitude observer is lost when the velocity goes to zero.

Remark 1: For this setup we have assumed available AHRS measurements. Although, an equivilant setup is possible in the body-frame with observers from Theorem 2, if a gravity vector estimate is available in body-frame as in [9].

A. Position estimate

As we have no knowledge of absolute position, we will only care about relative position change. The position estimate is derived from the estimated relative position vectors

$$
\hat{\boldsymbol{p}}^n(t) = \sum_{i=1}^m w_i(t)(\hat{\boldsymbol{\delta}}_i^n(0) - \hat{\boldsymbol{\delta}}_i^n(t)) \tag{68}
$$

where w_i are gains that sum up to one $\sum_{i=1}^m w_i = 1$. The estimate of the pose will converge as the relative position vector estimates converge, although there will be a constant offset due to the initial position estimate error

B. Simulation Results

The observer was tested in simulations. The scenario presented in this section is a vehicle travelling in a circle in 3D-space at constant velocity $\boldsymbol{v}^b = [0.5,\ 0,\ 0][m/s]$. The trajectory of the vessel, with the landmarks positions, can be seen in Figure 3. The simulator is implemented using Euler integration, having step length $h = 0.025[s]$ and lasts for

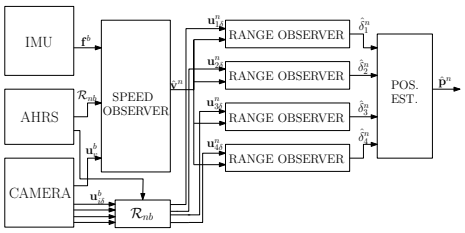

Fig. 2: Block diagram of the cascade structure of the speed observer (66) and range observer (67), for Bearing Only SLAM with 4 landmarks

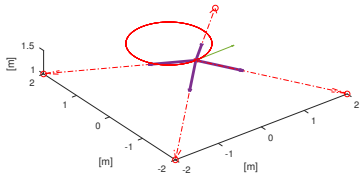

Fig. 3: The figure shows the trajectory of the vehicle, and the landmarks. The green arrow represent the normalized velocity measurement; the blue arrows represent the LOS measurements; the red dashed arrows represent the estimated distance vectors using $\frac{1}{\hat{d}_{xi}}\hat{\boldsymbol{u}}^n_{xi}$ at the end of the simulation.

$40[s]$. Four landmarks were placed in the corners of a box with sides of $4[m]$. The IMU measurements were corrupted by white noise with standard deviation $\boldsymbol{\sigma}_\omega = \boldsymbol{I}0.02[rad/s]$ and $\boldsymbol{\sigma}_f = \boldsymbol{I}0.02[m/s^2]$, which is meant to resemble a low cost MEMS IMU. The noise in the bearing measurements was $\boldsymbol{\sigma}_u = \boldsymbol{I}0.00314[rad]$, resembeling a pixel error for a camera with 90^o field of view and 500 pixels image height/width; the AHRS noise was $\boldsymbol{\sigma}_{\mathcal{R}} = \boldsymbol{I}0.0116[rad]$ giving a 3σ value of 2^o; the velocity direction had a white noise of $\boldsymbol{\sigma}_v = \boldsymbol{I}0.1060[rad]$, which is what you can expect from a Homography with the above image [9]. The bearing noise is orthogonal to the bearing $\boldsymbol{u}_n = \boldsymbol{S}(\boldsymbol{u}^n_x)\boldsymbol{w}_u$, in which the noise $\boldsymbol{w}_u$ is a white noise vector $\boldsymbol{w}_u = \mathcal{N}(0, \boldsymbol{\sigma}_u)$, the same is applied to the noise of the normalized velocity.

The speed observer was tuned with $k_v = 2\sqrt{\alpha}$ and $\gamma_v = \alpha/\|\mathcal{B}_u(t)\|$, with $\alpha = 0.5$. The range observers were tuned with $k_{\delta i} = 2\sqrt{2}$ and $\gamma_{\delta i} = 2$. The tuning is based on [21]. The observers were also implemented using the Euler method with $h = 0.025[s]$; the unit vector estimates should be normalized for every iteration to compensate for numerical errors. In Figure 4, we note that since the acceleration input is found by subtracting the gravity from the rotated specific force, most of the noise comes from the noisy attitude measurements. In Figure 5 we see how the velocity direction estimates are smooth compared to the measurents. Further, in Figure 6 we see how the velocity magnitude estimate converges, and in Figures 7 and 8 we see how the range and position estimates converge; this confirms that the observers can be used in cascade.

The authors still want to emphasise that there are assumptions for this scenario which are often broken when bearing only SLAM is used. The landmarks are assumed to be observed for the entire period; the attitude is only corrupted by white noise, so gravity is removed from the specific force.

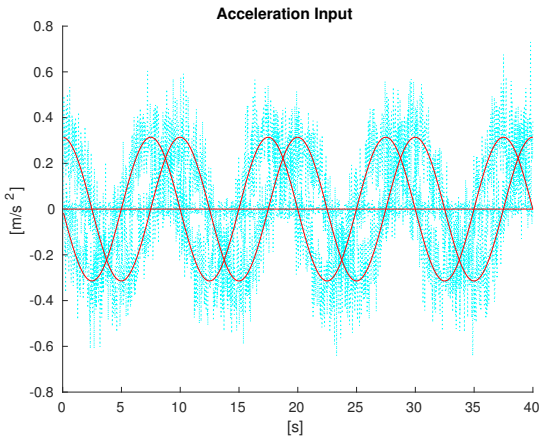

Fig. 4: The figure shows the acceleration input to the velocity magnitude observer. The red is the true acceleration, and the blue is the input for the velocity observer.

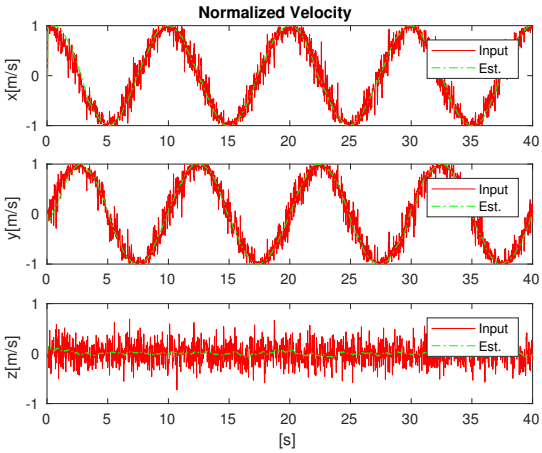

Fig. 5: The figure show the normalized velocity, in combination with the velocity direction estimate.

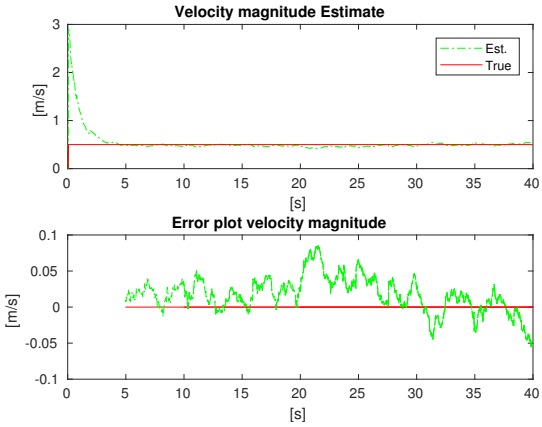

Fig. 6: The upper plot shows the velocity magnitude estimate combined with the true norm of the velocity, while the bottom plot shows the velocity error

However, the setup is able to estimate the position of the vessel, and the distance to the landmarks by only having IMU, AHRS, bearing and optical flow measurements, and without dead reckoning. This also shows the duality between the range estimation problem, and speed estimation problem; implying that other globally stable observers can be used for velocity estimation fusing camera with IMU and AHRS data [7], [8], [11], making velocity measurements redundant.

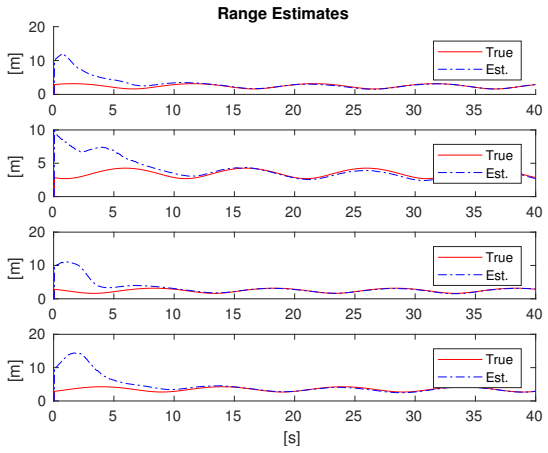

Fig. 7: The figure shows the range estimates and true ranges for the 4 landmarks

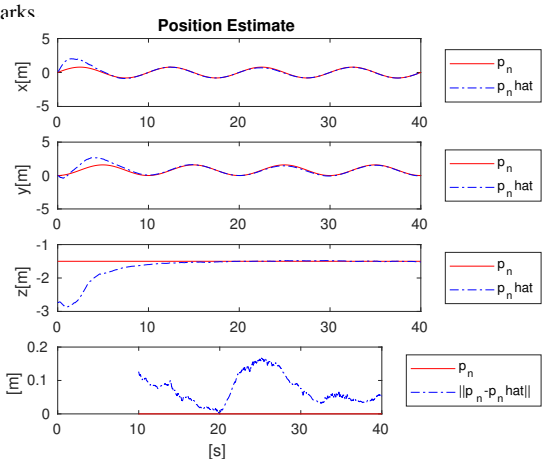

Fig. 8: The figure shows the position estimates for x, y and z direction, and the lowermost plot shows the norm of the position error. To make comparison between the position estimate and the true position easier, the position estimate is shifted so that there is zero position error at time $t = 20[s]$

V. CONCLUSION

We presented a novel vector magnitude observer, which uses unit vector measurement and derivative. The observer was proven to be uniformly semi-globally stable (USGAS) and UES in a defined region, moreover, the stability was of multiple instances, and in cascade. The vector magnitude framework was then applied to a bearing-only SLAM filter problem with AHRS, which demonstrated the filtering properties and convergence of the observer. This also demonstrated how a velocity estimation could be performed with camera, IMU and AHRS, making velocity measurement possibly redundant when these sensors are available.

ACKNOWLEDGEMENT

This work was supported by the Research Council of Norway through project number 250725 and project number 223254. Also thanks to Torleiv H. Bryne and Antonio Loria for helpful discussion on the proof.

REFERENCES

[1] R. Hartley and A. Zisserman, *Multiple view geometry in computer vision*. Cambridge university press, 2003.
[2] D. Nistér, "An Efficient Solution to the Five-Point Relative Pose Problem," *IEEE transactions on pattern analysis and machine intelligence*, vol. 26, no. 6, pp. 756–770, 2004.
[3] S. Weiss, R. Brockers, and L. Matthies, "4DoF drift free navigation using inertial cues and optical flow," in *IEEE International Conference on Intelligent Robots and Systems*, pp. 4180–4186, 2013.
[4] A. I. Mourikis and S. I. Roumeliotis, "A Multi-State Constraint Kalman Filter for Vision-aided Inertial Navigation," in *Proceedings 2007 IEEE International Conference on Robotics and Automation*, (Rome, Italy), pp. 3565–3572, IEEE, apr 2007.
[5] G. Grisetti, R. Kummerle, C. Stachniss, and W. Burgard, "A tutorial on graph-based SLAM," *IEEE Intelligent Transportation Systems Magazine*, vol. 2, no. 4, pp. 31–43, 2010.
[6] K. E. Bekris, M. Glick, and L. E. Kavraki, "Evaluation of algorithms for bearing-only slam," in *Robotics and Automation, 2006. ICRA 2006. Proceedings 2006 IEEE International Conference on*, pp. 1937–1943, IEEE, 2006.
[7] E. Bjorne, T. A. Johansen, and E. F. Brekke, "Redesign and analysis of globally asymptotically stable bearing only SLAM," in *2017 20th International Conference on Information Fusion (Fusion)*, pp. 1–8, IEEE, jul 2017.
[8] P. Lourenço, B. J. Guerreiro, P. Batista, P. Oliveira, and C. Silvestre, "3-d inertial trajectory and map online estimation: Building on a GAS sensor-based SLAM filter," in *Control Conference (ECC), 2013 European*, pp. 4214–4219, IEEE, 2013.
[9] V. Grabe, H. H. Bülthoff, D. Scaramuzza, and P. R. Giordano, "Nonlinear ego-motion estimation from optical flow for online control of a quadrotor UAV," *The International Journal of Robotics Research*, vol. 34, no. 8, pp. 1114–1135, 2015.
[10] M. Jankovic and B. K. Ghosh, "Visually guided ranging from observations of points, lines and curves via an identifier based nonlinear observer," *Systems & Control Letters*, vol. 25, no. 1, pp. 63–73, 1995.
[11] F. Le Bras, T. Hamel, R. Mahony, and C. Samson, "Observers for position estimation using bearing and biased velocity information," in *Sensing and Control for Autonomous Vehicles*, pp. 3–23, Springer, 2017.
[12] M. Kristic, I. Kanellakopulos, and P. V. Kokotovic, *Nonlinear And Adaptive control Design*. Wiley, 1995.
[13] H. K. Khalil, *Nonlinear Systems*. Prentice Hall, 2002.
[14] A. Loría and E. Panteley, "cascaded nonlinear time-varying systems: Analysis and design," in *Advanced topics in control systems theory*, pp. 23–64, Springer, 2005.
[15] A. Chaillet and A. Loría, "Uniform semiglobal practical asymptotic stability for non-autonomous cascaded systems and applications," *Automatica*, vol. 44, no. 2, pp. 337–347, 2008.
[16] H. Sussmann and P. Kokotovic, "The peaking phenomenon and the global stabilization of nonlinear systems," *IEEE Transactions on automatic control*, vol. 36, no. 4, pp. 424–440, 1991.
[17] H. Durrant-Whyte and T. Bailey, "Simultaneous localization and mapping(SLAM): part i," *IEEE robotics & automation magazine*, vol. 13, no. 2, pp. 99–110, 2006.
[18] T. Bailey and H. Durrant-Whyte, "Simultaneous localization and mapping(SLAM): Part ii," *IEEE Robotics & Automation Magazine*, vol. 13, no. 3, pp. 108–117, 2006.
[19] H. F. Grip, T. I. Fossen, T. A. Johansen, and A. Saberi, "Attitude estimation using biased gyro and vector measurements with time-varying reference vectors," *IEEE Transactions on Automatic Control*, vol. 57, no. 5, pp. 1332–1338, 2012.
[20] C. Forster, M. Pizzoli, and D. Scaramuzza, "Svo: Fast semi-direct monocular visual odometry," in *Robotics and Automation (ICRA), 2014 IEEE International Conference on*, pp. 15–22, IEEE, 2014.
[21] R. Spica and P. R. Giordano, "A framework for active estimation: Application to structure from motion," in *Proceedings of the IEEE Conference on Decision and Control*, pp. 7647–7653, 2013.